

1           **A total energy error analysis of dynamical cores and**  
2           **physics-dynamics coupling in the Community Atmosphere**  
3           **Model (CAM)**

4           **Peter H. Lauritzen<sup>1\*</sup>, and David L. Williamson<sup>1</sup>**

5           <sup>1</sup>National Center for Atmospheric Research, Boulder, Colorado, USA

6           **Key Points:**

- 7           • Spurious total energy dissipation in dynamical core is  $-0.3W/m^2$  to  $-1W/m^2$  at 1  
8           degree  
9           • Constant-pressure assumption in physics leads to  $0.3W/m^2$  spurious total energy  
10          source  
11          • There can easily be compensating errors in total energy budget

---

\*1850 Table Mesa Drive, Boulder, Colorado, USA

Corresponding author: Peter Hjort Lauritzen, pel@ucar.edu

12 **Abstract**

13 A closed total energy (TE) budget is of utmost importance in coupled climate system  
 14 modeling; in particular, the dynamical core or physics-dynamics coupling should ideally  
 15 not lead to spurious TE sources/sinks. To assess this in a global climate model, a detailed  
 16 analysis of the spurious sources/sinks of TE in NCAR's Community Atmosphere Model  
 17 (CAM) is given. This includes spurious sources/sinks associated with the parameteriza-  
 18 tion suite, the dynamical core, TE definition discrepancies and physics-dynamics coupling.  
 19 The latter leads to a detailed discussion of the pros and cons of various physics-dynamics  
 20 coupling methods commonly used in climate/weather modeling.

21 **1 Introduction**

22 In coupled climate modeling with prognostic atmosphere, ocean, land, land-ice, and  
 23 sea-ice components, it is important to conserve total energy (TE) to a high degree in each  
 24 component individually and in the complete model to avoid spurious long term trends in  
 25 the simulated Earth system. Conservation of TE in this context refers to having a closed  
 26 TE budget. For example, the TE change in a column in the atmosphere is exactly balanced  
 27 by the net sources/sinks given by the fluxes through the column. The fluxes into the at-  
 28 mospheric component from the surface models must be balanced by the fluxes in the re-  
 29 spective surface components and so on. Henceforth we will focus only on the atmospheric  
 30 component which, in a numerical model, is split into a resolved-scale component (the dy-  
 31 namical core) and a sub-grid-scale component (parameterizations or, in modeling jargon,  
 32 physics). While there have been many studies on energy flow in the Earth system through  
 33 analysis of re-analysis data and observations [Trenberth and Fasullo, 2018, and references  
 34 herein], there has been less focus on spurious TE sources/sinks in numerical models.

35 The atmospheric equations of motion conserve TE but the discretizations used in cli-  
 36 mate and weather models are usually not inherently TE conservative. Exact conservation  
 37 is probably not necessary but conservation to within  $\sim 0.01 \text{ W/m}^2$  has been considered  
 38 sufficient to avoid spurious trends in century long simulations [Boville, 2000; Williamson  
 39 *et al.*, 2015]. Spurious sources and sinks of TE can be introduced by the dynamical core,  
 40 physics, physics-dynamics coupling as well as discrepancies between the TE of the con-  
 41 tinuous and discrete equations of motion and for the physics. Hence the study of TE con-  
 42 servation in comprehensive models of the atmosphere quickly becomes a quite complex  
 43 and detailed matter. In addition there can easily be compensating errors in the system as a  
 44 whole.

45 Here we focus on versions of the Community Atmosphere Model (CAM) that use  
 46 the spectral-element [SE, Lauritzen *et al.*, 2018] and finite-volume [FV, Lin, 2004] dy-  
 47 namical cores. These dynamical cores couple with physics in a time-split manner, i.e.  
 48 physics receives a state updated by dynamics [see Williamson, 2002, for a discussion  
 49 of time-split versus process split physics-dynamics coupling in the context of CAM]. In  
 50 its pure time-split form the physics tendencies are added to the state previously produced  
 51 by the dynamical core and the resulting state provides the initial state for the subsequent  
 52 dynamical core calculation. We refer to this as *state-updating* (`ftype=1` in CAM code).  
 53 Alternatively, when the dynamical core adopts a shorter time step than the physics, say  
 54 `nsplit` sub-steps, then  $(1/\text{nsplit})$ th of the physics-calculated tendency is added to the  
 55 state before each dynamics sub-step. We refer to this modification of time-splitting as  
 56 *dribbling* (`ftype=0`). CAM-FV uses the *state-update* (`ftype=1`) approach while CAM-SE  
 57 has options to use *state-update* (`ftype=1`), *dribbling* (`ftype=0`) or a combination of the  
 58 two i.e. mass-variables use *state-updating* and remaining variables use *dribbling*. We refer  
 59 to this as *combination* (`ftype=2`). The *dribbling* variants can lead to spurious sources or  
 60 sinks of TE (and mass) referred to here as physics-dynamics coupling errors.

61 The dynamical core usually has inherent or specified filters to control spurious noise  
 62 near the grid scale which will lead to energy dissipation [Thuburn, 2008; Jablonowski

and Williamson, 2011]. Similarly models often have sponge layers to control the solution near the top of the model that may be a sink of TE. There are examples of numerical discretizations of the adiabatic frictionless equations motion that are designed so that TE is conserved in the absence of time-truncation and filtering errors [e.g., Eldred and Randall, 2017; McRae and Cotter, 2013], e.g., mimetic spectral-element discretizations such as the one used in the horizontal in CAM-SE [Taylor, 2011]. These provide consistency between the discrete momentum and thermodynamic equations leading to global conservation associated with the conversion of potential to kinetic energy. In spectral transform models it is customary to add the energy change due to explicit diffusion on momentum back as heating (referred to as frictional heating), so that the diffusion of momentum does not affect the TE budget [see, e.g., p.71 in Neale et al., 2012]. This is also done in CAM-SE [Lauritzen et al., 2018].

The purpose of this paper is to provide a detailed global TE analysis of CAM. We assess TE errors due to various steps in the model algorithms. The paper is outlined as follows. In section 2 the continuous TE formulas are given and a detailed description of spurious TE sources/sinks that can occur in a model as a whole, and the associated diagnostics used to perform the TE analysis, are defined. In section 3 the model is run in various configurations to assess their effects on TE conservation. This includes various physics-dynamics coupling experiments leading to a rather detailed discussion of mass budget closure. We also investigate the effect of using a limiter in the vertical remapping of momentum, assess energy discrepancy errors and impacts on TE of simplifying surface conditions and dry atmosphere experiments. The paper ends with conclusions.

## 2 Method

### 2.1 Defining total energy (TE)

In the following it is assumed that the model top and bottom are coordinate surfaces and that there is no flux of mass through the model top and bottom. In a dry atmosphere the TE equation integrated over the entire sphere is given by

$$\frac{d}{dt} \int_{z=z_s}^{z=z_{top}} \iint_S E_v \rho^{(d)} dA dz = \int_{z=z_s}^{z=z_{top}} \iint_S F_{net} \rho^{(d)} dA dz, \quad (1)$$

[e.g., Kasahara, 1974] where  $F_{net}$  is net flux calculated by the parameterizations (e.g., heating and momentum forcing),  $d/dt$  the total/material derivative,  $z_s$  is the height of the surface,  $S$  the sphere,  $\rho^{(d)}$  the density of dry air,  $E_v$  is the TE and  $dA$  is an infinitesimal area on the sphere.  $E_v$  can be split into kinetic energy  $K = \frac{1}{2}\mathbf{v}^2$  ( $\mathbf{v}$  is the wind vector), internal energy  $c_v^{(d)}T$ , where  $c_v^{(d)}$  is the heat capacity of dry air at constant volume, and potential energy  $\Phi = gz$

$$E_v = K + c_v^{(d)}T + \Phi. \quad (2)$$

If the vertical integral is performed in a mass-based vertical coordinate, e.g., pressure, then the integrated TE equation for a dry atmosphere can be written as

$$\frac{d}{dt} \int_{p=p_s}^{p=p_{top}} \iint_S E_p \rho^{(d)} dA dp + \frac{d}{dt} \iint_S \Phi_s p_s dA = \int_{p=p_s}^{p=p_{top}} \iint_S F_{net} \rho dA dp, \quad (3)$$

[e.g., Kasahara, 1974] where

$$E_p = K + c_p^{(d)}T. \quad (4)$$

In a moist atmosphere, however, there are several definitions of TE used in the literature related to what heat capacity is used for water vapor and whether or not condensates are accounted for in the energy equation. To explain the details of that we focus on the energy equation for CAM-SE.

CAM-SE is formulated using a terrain-following hybrid-sigma vertical coordinate  $\eta$  but the coordinate levels are defined in terms of dry air mass per unit area ( $M^{(d)}$ ) instead of total air mass;  $\eta^{(d)}$  [see Lauritzen et al., 2018, for details]. In such a coordinate

106 system it is convenient to define the tracer state in terms of a dry mixing ratio instead of  
 107 moist mixing ratio

$$m^{(\ell)} \equiv \frac{\rho^{(\ell)}}{\rho^{(d)}}, \text{ where } \ell = 'wv', 'cl', 'ci', 'rn', 'sw', \quad (5)$$

108 where  $\rho^{(d)}$  is the mass of dry air per unit volume of moist air and  $\rho^{(\ell)}$  is the mass of the  
 109 water substance of type  $\ell$  per unit volume of moist air. Moist air refers to air containing  
 110 dry air ('d'), water vapor ('wv'), cloud liquid ('cl'), cloud ice ('ci'), rain amount ('rn')  
 111 and snow amount ('sw'). For notational purposes define the set of all components of air

$$\mathcal{L}_{all} = \{'d', 'wv', 'cl', 'ci', 'rn', 'sw'\}, \quad (6)$$

112 Define associated heat capacities at constant pressure  $c_p^{(\ell)}$ . How many and which con-  
 113 densates are thermodynamically active in the dynamical core is controlled with namelist  
 114 `qsize_condensate_loading`. If `qsize_condensate_loading=1` only water vapor  
 115 ('wv') is active, `qsize_condensate_loading=3` 'wv', 'cl', and 'ci' are active, and if  
 116 `qsize_condensate_loading=5` then 'wv', 'cl', 'ci', 'rn', and 'sw' are included.

117 Using the  $\eta^{(d)}$  vertical coordinate and dry mixing ratios the TE (per unit area) that  
 118 the frictionless adiabatic equations of motion in the CAM-SE dynamical core conserves is

$$\widehat{E}_{dyn} = \frac{1}{\Delta S} \int_{\eta=0}^{\eta=1} \iint_S \left( \frac{1}{g} \frac{\partial M^{(d)}}{\partial \eta^{(d)}} \right) \sum_{\ell \in \mathcal{L}_{all}} [m^{(\ell)} (K + c_p^{(\ell)} T + \Phi_s)] dA d\eta^{(d)}, \quad (7)$$

119 where  $\Delta S$  is the surface area of the sphere,  $\Phi_s$  is the surface geopotential and  $\widehat{(\cdot)}$  refers to  
 120 the global average.

121 In the CAM physical parameterizations a different definition of TE is used. Due to  
 122 the evolutionary nature of the model development, the parameterizations have not yet been  
 123 converted to match the SE dynamical core. For the computation of TE, condensates are  
 124 assumed to be zero and the heat capacity of moisture is the same as for dry air. This is  
 125 equivalent to using a moist mass (dry air plus water vapor) but  $c_p$  of dry air:

$$\widehat{E}_{phys} = \frac{1}{\Delta S} \int_{\eta=0}^{\eta=1} \iint_S \left( \frac{1}{g} \frac{\partial M^{(d)}}{\partial \eta^{(d)}} \right) (1 + m^{(wv)}) [(K + c_p^{(d)} T + \Phi_s)] dA d\eta^{(d)}. \quad (8)$$

126 We note that earlier versions of CAM using the spectral transform dynamical core used  
 127  $c_p$  of moist air. The adiabatic, frictionless equations of motion in the CAM-SE dynamical  
 128 core can be made consistent with  $E_{phys}$  by not including condensates in the mass/pressure  
 129 field as well as energy conversion term in the thermodynamic equation and setting the  
 130 heat capacity for moisture to  $c_p^{(d)}$  [Taylor, 2011]. We refer to this version of CAM-SE as  
 131 the *energy consistent* version.

## 132 2.2 Spurious energy sources and sinks

133 In a weather/climate model TE conservation errors can appear in many places through-  
 134 out the algorithm. Below is a general list of where conservation errors can appear with  
 135 specific examples from CAM:

- 136 1. *Parameterization errors*: Individual parameterizations may not have a closed en-  
 137 ergy budget. CAM parameterizations are required to have a closed energy budget  
 138 under the assumption that pressure remains constant during the computation of the  
 139 subgrid-scale parameterization tendencies. In other words, the TE change in the  
 140 column is exactly balanced by the net sources/sinks given by the fluxes through the  
 141 column.
- 142 2. *Pressure work*: That said, if parameterizations update specific humidity then the  
 143 surface pressure changes (e.g., moisture entering or leaving the column). In that

- case the pressure changes which, in turn, changes TE. This is referred to as *pressure work* [section 3.1.8 in *Neale et al.*, 2012].
3. *Continuous TE formula discrepancy*: If the continuous equations of motion for the dynamical core conserve a TE different from the one used in the parameterizations then an energy inconsistency is present in the system as a whole. This is the case with the new version of CAM-SE that conserves a TE that is more accurate and comprehensive than that used in the CAM physics package as discussed above. As also noted above, this mismatch arose from the evolutionary nature of the model development and not by deliberate design; and should be eliminated in the future.
  4. *Dynamical core errors*: Energy conservation errors in the dynamical core, not related to physics-dynamics coupling errors, can arise in multiple parts of the algorithms used to solve the equations of motion. For dynamical cores employing filtering [e.g., limiters in flux operators *Lin*, 2004] and/or possessing inherent damping which controls small scales, it is hard to isolate their energy dissipation from other errors in the discretization. If a hyperviscosity term or some other diffusion is added to the momentum equation, then one can diagnose the local energy dissipation from such damping and add a corresponding heating to balance it (frictional heating). There may also be energy loss from viscosity applied to other variables such as temperature or pressure which is harder to compensate. Here is a break-down relevant to CAM-SE using a floating Lagrangian vertical coordinate:
    - Horizontal inviscid dynamics: Energy errors resulting from solving the inviscid, adiabatic equations of motion.
    - Hyperviscosity: Filtering errors.
    - Vertical remapping: The vertical remapping algorithm from Lagrangian to Eulerian reference surfaces does not conserve TE.
    - Near round-off negative values of water vapor which are filled to a minimal value without compensation.
  5. *Physics-dynamics coupling (PDC)*: Assume that physics computes a tendency. Usually the tendency (forcing) is passed to the dynamical core which is responsible for adding the tendencies to the state. PDC energy errors can be split into three types:
    - *'Dribbling' errors (or, equivalently, temporal PDC errors)*: If the TE increment from the parameterizations does not match the change in TE when the tendencies are added to the state in the dynamical core, then there will be a spurious PDC error. This will not happen with the *state-update* approach in which the tendencies are added immediately after physics and before the dynamical core advances the solution in time.
    - *Change of vertical grid/coordinate errors*: If the vertical coordinates in physics and in the dynamical core are different then there can be spurious PDC energy errors even when using the state-update method for adding tendencies to the dynamical core state. For example, many non-hydrostatic dynamical cores [e.g. *Skamarock et al.*, 2012] use a terrain-following height coordinate whereas physics uses pressure.
    - *Change of horizontal grid errors*: If the physics tendencies are computed on a different horizontal grid than the dynamical core then there can be spurious energy errors from mapping tendencies and/or variables between horizontal grids [e.g., *Herrington et al.*, 2018].
  6. *Compensating Energy fixers*: To avoid TE conservation errors which could accumulate and ultimately lead to a climate drift, it is customary to apply an arbitrary energy fixer to restore TE conservation. Since the spatial distribution of many energy errors, in general, is not known, global fixers are used. In CAM a uniform increment is added to the temperature field to compensate for TE imbalance from all processes, i.e. dynamical core, physics-dynamics coupling, TE formula discrep-

196       ancy, energy change due to pressure work, and possibly parameterization errors if  
 197       present.

198       **2.3 Diagnostics**

199       The discrete global averages  $\widehat{(\cdot)}$  are computed consistent with the discrete model  
 200       grid as outlined in section 2.2. of *Lauritzen et al. [2014]*. The TE global average tendency  
 201       is denoted

$$\partial \widehat{E} \equiv \frac{d \widehat{E}}{dt}. \quad (9)$$

202       By computing the global TE averages  $\widehat{E}$  at appropriate places in the model algorithms, we  
 203       can directly compute  $\partial \widehat{E}$  due to various processes (such as viscosity, vertical remapping,  
 204       physics-dynamics coupling, pressure work, etc.) by differencing  $\widehat{E}$  from after and before  
 205       the algorithm takes place. This has been implemented using CAM history infrastructure  
 206       by computing column integrals of energy at various places in CAM and outputting the 2D  
 207       energy fields. CAM history internally handles accumulation and averaging in time at each  
 208       horizontal grid point. The global averages are computed externally from the grid point  
 209       vertical integrals on the history files (stored in double precision). The places in CAM  
 210       where we compute/capture the grid point vertical integral  $E$  are named using three letters  
 211       where the first letter refers to whether the vertical integral is performed in physics ('p') or  
 212       in the dynamical core ('d'). The trailing two letters refer to the specific location in dynam-  
 213       ics or physics. For example, 'BP' refers to 'Before Physics' and 'AP' to 'After Physics';  
 214       the associated total energies are denoted  $E_{pBP}$  and  $E_{pAP}$ , respectively. The TE tendency  
 215       from the parameterizations is the difference between  $E_{pBP}$  and  $E_{pAP}$  divided by the time-  
 216       step. The terms and tendencies are then averaged globally externally to the model. The  
 217       pseudo-code in Figure 1 defines the acronyms in terms of where in the CAM-SE algo-  
 218       rithm the TE vertical integrals are computed and output. For details on the CAM-SE algo-  
 219       rithm please see *Lauritzen et al. [2018]*.

220       Before defining the individual terms in detail we briefly review the model time step-  
 221       ping sequence starting with the physics component as illustrated in Figure 1. The energy  
 222       fixer is applied first to compensate for the spurious net energy change from all compo-  
 223       nents introduced during the previous time step. We will describe this in more detail af-  
 224       ter the various sources and sinks are elucidated. The parameterizations are applied next  
 225       and are required to be energy conserving. They update the state and accumulate the total  
 226       physics tendency (forcing). At this stage the state is saved for use in the energy fixer in  
 227       the next time step. Any changes in the global average energy after this are spurious and  
 228       are compensated by the fixer. The parameterizations update the water vapor but not the  
 229       moist pressure, implying a non-physical change in the dry mass of the atmosphere. The  
 230       dry mass correction corrects the dry mass back to its proper value.

231       The forcing (physics tendency) from the parameterizations is passed to the dynam-  
 232       ical core. If the physics and dynamics operate on different grids, the forcing is remapped  
 233       here. The dynamics operates on a shorter time step than the physics and is sub-stepped. The  
 234       remapped forcing is applied to the dynamics state, saved from the end of the previous  
 235       dynamics step, using either *state-updating*, *dribbling*, or *combination* as described in the  
 236       introduction. The dynamics then advances the adiabatic frictionless flow in the floating  
 237       Lagrangian layers over a further set of sub-steps. Hyperviscosity is applied next with fur-  
 238       ther sub-stepping required for computational stability of the explicit discrete approxima-  
 239       tions. The energy loss from the specified momentum viscosity is calculated locally and is  
 240       balanced by adding a local change to the temperature, referred to as *frictional heating*.  
 241       This set of dynamics sub-steps is followed by the vertical remapping from Lagrangian to  
 242       Eulerian reference layers. The remapping is required to provide layers consistent with the  
 243       parameterization formulations. The vertical remapping sub-steps are required for stability  
 244       if the Lagrangian layers become too thin.

At the end of the dynamics, the state is saved to be used by the dynamics the next time step and is also passed to the physics, with a remapping if the dynamics and physics grids differ. At the beginning of the physics the difference in energy between this state and the state saved after the physics during the previous time step is the amount needed to be added or subtracted by the energy fixer. It represents the accumulation of all spurious sources from the dry mass correction, remappings between physics and dynamics grids (if applicable), dynamical core, differing energy definitions (if present), hyerviscosity, and vertical remapping.

We now define the following energy tendencies corresponding to the itemized list in section 2.2 with references to terms indicated in Figure 1. We start just after the energy fixer which will be defined at the end.

1.  $\partial\widehat{E}^{(param)}$ : TE tendency due to parameterizations. In CAM the TE budget for each parameterization is closed (assuming pressure is unchanged) so  $\partial\widehat{E}^{(param)}$  is balanced by net fluxes in/out of the physics columns. Note that this is the only energy tendency that is not spurious since CAM parameterizations have a closed TE budget. This TE tendency is discretely computed as

$$\partial\widehat{E}_{phys}^{(param)} = \frac{\widehat{E}_{pAP} - \widehat{E}_{pBP}}{\Delta t_{phys}}, \quad (10)$$

where  $\Delta t_{phys}$  is the physics time-step (default 1800s) and the subscript *phys* on  $\partial\widehat{E}$  refers to the energy tendency computed in CAM physics.

2.  $\partial\widehat{E}^{(pwork)}$ : Total spurious energy tendency due to pressure work

$$\partial\widehat{E}_{phys}^{(pwork)} = \frac{\widehat{E}_{pAM} - \widehat{E}_{pAP}}{\Delta t_{phys}}. \quad (11)$$

Since CAM-SE dynamical core is based on a dry-mass vertical coordinate the pressure work takes place implicitly in the dynamical core. But the TE tendency due to pressure work is conveniently computed in physics since dynamical cores based on a moist vertical coordinate (e.g., CAM-FV) require pressure and moist mixing ratios to be adjusted for dry mass conservation and tracer mass conservation [section 3.1.8 in *Neale et al., 2012*]. The difference of TE after and before this adjustment is the TE tendency due to pressure work. In a dry mass vertical coordinate based on dry mixing ratios neither dry mass layer thickness nor dry mixing ratios need to be adjusted to take into account moisture changes in the column. For labeling purposes, the 'total forcing' associated with physics (at least in CAM) consists of parameterizations, pressure work and TE fixer, although strictly speaking the fixer includes components from the dynamics as will be seen.

$$\partial\widehat{E}_{phys}^{(phys)} \equiv \partial\widehat{E}_{phys}^{(param)} + \partial\widehat{E}_{phys}^{(pwork)} + \partial\widehat{E}_{phys}^{(efix)} = \frac{\widehat{E}_{pAM} - \widehat{E}_{pBF}}{\Delta t_{phys}}. \quad (12)$$

where the energy fixer TE tendency is

$$\partial\widehat{E}_{phys}^{(efix)} = \frac{\widehat{E}_{pBP} - \widehat{E}_{pBF}}{\Delta t_{phys}}. \quad (13)$$

After all the TE budget terms have been defined, the exact composition of  $\partial\widehat{E}_{phys}^{(efix)}$  will be presented.

3.  $\partial\widehat{E}^{(discr)}$ : If the physics uses a TE definition different from the TE that the continuous equations of motion in the dynamical core conserve (i.e. in the absence of discretization errors), then there is a TE discrepancy tendency. This complicates the energy analysis as one can not compare TE computed in physics  $\widehat{E}_{phys}$  directly with TE computed in the dynamical core  $\widehat{E}_{dyn}$ . This makes errors associated with

this discrepancy tricky to assess. That said, the TE tendencies computed using the dynamical core TE formula  $\partial\widehat{E}_{dyn}$  are well defined (self consistent) and similarly for TE tendencies computed using the ‘physics formula’ for TE,  $\partial\widehat{E}_{phys}$ .

- 295 4. The TE tendency from the dynamical core is split into several terms: Horizontal  
296 adiabatic dynamics (dynamics excluding physics forcing tendency)

$$\partial\widehat{E}_{dyn}^{(2D)} = \frac{\widehat{E}_{dAD} - \widehat{E}_{dBH}}{\Delta t_{dyn}}, \quad (14)$$

297 where over a single dynamics sub-step  $\Delta t_{dyn} = \frac{\Delta t_{phys}}{n_{split} \times r_{split}}$  (the loop bounds  
298  $n_{split}$ ,  $r_{split}$ , etc. are explained in Figure 1).

299 In CAM-SE the viscosity is explicit so one can compute the TE tendency due to  
300 hyperviscosity and its associated frictional heating

$$\partial\widehat{E}_{dyn}^{(hvis)} = \frac{\widehat{E}_{dAH} - \widehat{E}_{dBH}}{\Delta t_{hvis}}, \quad (15)$$

301 which, in CAM-SE, includes a frictional heating term from viscosity on momentum

$$\partial\widehat{E}_{dyn}^{(fheat)} = \frac{\widehat{E}_{dAH} - \widehat{E}_{dCH}}{\Delta t_{hvis}}, \quad (16)$$

302 where  $\Delta t_{hvis} = \frac{\Delta t_{phys}}{n_{split} \times r_{split} \times h_{hypervis\_subcycle}}$  is the time step of the sub-stepped  
303 viscosity. The residual

$$\partial\widehat{E}_{dyn}^{(res)} = \partial\widehat{E}_{dyn}^{(2D)} - \partial\widehat{E}_{dyn}^{(hvis)}, \quad (17)$$

304 is the energy error due to inviscid dynamics and time-truncation errors.

305 The energy tendency due to vertical remapping is

$$\partial\widehat{E}_{dyn}^{(remap)} = \frac{\widehat{E}_{dAR} - \widehat{E}_{dAD}}{\Delta t_{remap}}, \quad (18)$$

306 where  $\Delta t_{remap} = \frac{\Delta t_{phys}}{n_{split}}$ .

307 The 3D adiabatic dynamical core (no physics forcing but including friction) energy  
308 tendency is denoted

$$\partial\widehat{E}_{dyn}^{(adiab)} = \partial\widehat{E}_{dyn}^{(2D)} + \partial\widehat{E}_{dyn}^{(remap)}. \quad (19)$$

- 309 5.  $\partial\widehat{E}^{(pdc)}$ : Total spurious energy tendency due to physics-dynamics coupling errors  
310 is the difference between the energy tendency from physics and the energy ten-  
311 dency in the dynamics resulting from adding the physics increment to the dynami-  
312 cal core state

$$\partial\widehat{E}^{(pdc)} = \partial\widehat{E}_{phys}^{(phys)} - \partial\widehat{E}_{dyn}^{(phys)} \text{ assuming } \partial\widehat{E}^{(discr)} = 0, \quad (20)$$

313 where

$$\partial\widehat{E}_{dyn}^{(phys)} = \frac{\widehat{E}_{dBH} - \widehat{E}_{dAF}}{\Delta t_{pdc}}, \quad (21)$$

314 and  $\Delta t_{pdc}$  is the time-step between physics increments being added to the dynami-  
315 cal core. Remember we are dealing with average rates so terms computed with dif-  
316 ferent time steps can be compared, but differences cannot be taken between terms  
317 sampled with different time steps.

318 The physics-dynamics coupling TE tendency  $\partial\widehat{E}^{(pdc)}$  makes use of TE formulas  
319 in dynamics and in physics so (20) is only well-defined if the TE formula discrep-  
320 ance is zero,  $\partial\widehat{E}^{(discr)} = 0$ . As mentioned in Section 2.1, CAM-SE has the op-  
321 tion to switch the continuous equations of motion conserving the TE used by CAM  
322 physics (8) instead of the more comprehensive TE formula (7).

323 In CAM-SE there are 3 physics-dynamics coupling algorithms described in detail  
324 in section 3.6 in *Lauritzen et al. [2018]* and reviewed in the introduction here. One

325 is *state-update* in which the entire physics increments are added to the dynamics  
 326 state at the beginning of dynamics (referred to as `ftype=1`), in which case  $\Delta t_{pdc} =$   
 327  $\Delta t_{phys}$ . Another is *dribbling* in which the physics tendency is split into `nsplit`  
 328 equal chunks and added throughout dynamics (more precisely after every vertical  
 329 remapping; referred to as `ftype=0` resulting in  $\Delta t_{pdc} = \frac{1}{nsp1t} \Delta t_{phys}$ ), and then a  
 330 *combination* of the two (referred to as `ftype=2`) where tracers (mass variables) use  
 331 *state-update* (`ftype=1`) and all other physics tendencies use *dribbling* (`ftype=0`).  
 332

- 333 6.  $\partial \widehat{E}^{(efix)}$ : Global energy fixer tendency, defined in (13), is applied at the beginning  
 334 of the parameterizations. The correction needed is the global average difference  
 335 between the state passed from the dynamics and the state that was saved after the  
 336 physics updated the state but before the dry mass correction. It includes all spu-  
 337 rious sources from the dry mass correction, remappings between physics and dy-  
 338 namics, dynamical core, differing energy definitions (if present), hyperviscosity, and  
 vertical remapping.

## 339 2.4 A few observations regarding the energy budget terms

340 It is useful to note that the energy fixer ‘fixes’ energy errors for the dynamical core,  
 341 pressure work, physics-dynamics coupling and TE discrepancy

$$-\partial \widehat{E}_{phys}^{(efix)} = \partial \widehat{E}_{phys}^{(pwork)} + \partial \widehat{E}_{dyn}^{(adiab)} + \partial \widehat{E}^{(pdc)} + \partial \widehat{E}^{(discr)}. \quad (22)$$

342 The forcing from the parameterizations,  $\partial \widehat{E}_{phys}^{(param)}$ , does not appear in this budget (al-  
 343 though the dynamical core state does ‘feel’ the parameterization forcing) as the energy  
 344 cycle for the parameterizations is, by design in CAM, closed (balanced by fluxes in/out of  
 345 the physics columns). If  $\partial \widehat{E}^{(discr)} = 0$ , one can use (22) to diagnose energy dissipation  
 346 in the dynamical core and physics-dynamics coupling from quantities computed only in  
 347 physics

$$\partial \widehat{E}_{dyn}^{(adiab)} + \partial \widehat{E}^{(pdc)} = -\partial \widehat{E}_{phys}^{(efix)} - \partial \widehat{E}_{phys}^{(pwork)} \text{ for } \partial \widehat{E}^{(discr)} = 0. \quad (23)$$

348 This is useful if the diagnostics are not implemented in the dynamical core; in particular,  
 349 if the *state-update* (`ftype=1`) physics-dynamics coupling method is used then  $\partial \widehat{E}^{(pdc)} = 0$   
 350 and the TE errors in the dynamical core can be computed without diagnostics imple-  
 351 mented in the dynamical core. Also, (23) provides an alternative formula for  $\partial \widehat{E}^{(pdc)}$   
 352 compared to (20):

$$\partial \widehat{E}^{(pdc)} = -\partial \widehat{E}_{phys}^{(efix)} - \partial \widehat{E}_{phys}^{(pwork)} - \partial \widehat{E}_{dyn}^{(adiab)} \text{ assuming } \partial \widehat{E}^{(discr)} = 0. \quad (24)$$

353 If  $\partial \widehat{E}^{(pdc)} = 0$  (22) can be used to compute  $\partial \widehat{E}^{(discr)}$

$$\partial \widehat{E}^{(discr)} = -\partial \widehat{E}_{phys}^{(efix)} - \partial \widehat{E}_{phys}^{(pwork)} - \partial \widehat{E}_{dyn}^{(adiab)}, \text{ assuming } \partial \widehat{E}^{(pdc)} = 0. \quad (25)$$

354 Note that we can not use (20) to compute  $\partial \widehat{E}^{(discr)}$  since  $\widehat{E}_{phys} \neq \widehat{E}_{dyn}$ .

## 355 3 Results

356 A series of simulations have been performed with CESM2.1 using CAM version 6  
 357 (CAM6) physics (<https://doi.org/10.5065/D67H1H0V>) on NCAR’s Cheyenne cluster  
 358 [*Computational and Information Systems Laboratory*, 2017]. All simulations are at nom-  
 359 inally  $\sim 1^\circ$  horizontal resolution (for CAM-SE that is  $30 \times 30$  elements on each cubed-  
 360 sphere face and for CAM-FV its  $192 \times 288$  latitudes-longitudes) and using the standard  
 361 32 levels in the vertical. Unless otherwise noted all simulations are 13 months in dura-  
 362 tion and the last 12 months are used in the analysis. Total energy budgets are summarized  
 363 in Table 1 and discussed below. The first column gives identifying ‘Descriptors’ which  
 364 are briefly summarized below and defined in more detail in the following sections. The  
 365 section titles also include the ‘Descriptor’ from Table 1 to make it easier for the reader

**Table 1.** TE tendencies in units of  $W/m^2$  associated with various aspects of CAM-SE run in AMIP-type setup (unless otherwise noted). Column 1 is the identifier for the model configuration. See the text for a brief summary of these descriptors. They are defined in more detail in the following sections where the section titles also include the ‘Descriptor’ from Table 1 to make it easier for the reader to match Table entries with discussion in the text. Column 2 is  $N = \text{qsizes\_condensate\_loading}$  identifying how many water species are thermodynamically active in the dynamical core (see section 2.1 for details). Column 3, `lcp_moist`, indicates whether or not the heat capacity includes water variables or not and column 4 shows physics-dynamics coupling method `ftype`. The TE tendencies  $\partial \widehat{E}$  in columns 5-14 are defined in section 2.3. If  $\partial \widehat{E}$  is less than  $10^{-5} W/m^2$  it is set to zero in the Table. Significant changes compared to the baseline (*TE consistent* configuration) discussed in the main text are in bold font.

Descriptor	$N$	<code>lcp_moist</code>	<code>ftype</code>	$\partial \widehat{E}_{\text{phys}}^{(\text{pwork})}$	$\partial \widehat{E}_{\text{phys}}^{(\text{efix})}$	$\partial \widehat{E}_{\text{phys}}^{(\text{discr})}$	$\partial \widehat{E}_{\text{dyn}}^{(2D)}$	$\partial \widehat{E}_{\text{dyn}}^{(hvis)}$	$\partial \widehat{E}_{\text{dyn}}^{(\text{fheat})}$	$\partial \widehat{E}_{\text{dyn}}^{(\text{res})}$	$\partial \widehat{E}_{\text{dyn}}^{(\text{remap})}$	$\partial \widehat{E}_{\text{dyn}}^{(\text{adiab})}$	$\partial \widehat{E}_{\text{dyn}}^{(\text{pdc})}$
<i>TE consistent</i>	1	false	1	0.312	0.300	0	-0.601	-0.608	0.565	0.007	-0.011	-0.613	0
‘dribbling’ A	1	false	0	0.315	0.313	0	<b>-0.577</b>	-0.584	0.568	0.007	-0.011	-0.588	<b>0.469</b>
‘dribbling’ B	1	false	2	0.316	0.341	0	-0.598	-0.606	0.563	0.008	-0.011	-0.609	<b>0.484</b>
<i>vert limiter</i>	1	false	1	0.317	0.472	0	-0.590	-0.597	0.509	0.006	<b>-0.199</b>	-0.789	0
<i>smooth topo</i>	1	false	1	0.315	<b>-0.008</b>	0	<b>-0.295</b>	<b>-0.300</b>	0.493	0.005	-0.012	<b>-0.307</b>	0
<i>energy discr</i>	5	true	1	0.332	-0.313	<b>0.594</b>	-0.603	-0.612	0.575	0.009	-0.011	-0.614	-
<i>default</i>	5	true	2	0.316	-0.272		-0.578	-0.587	0.579	0.010	-0.012	-0.589	-
<i>QPC6</i>	1	false	1	0.305	-0.169	0	<b>-0.129</b>	<b>-0.131</b>	0.477	0.001	-0.007	<b>-0.136</b>	0
<i>FHS94</i>	1	false	2	-	-	-	<b>-0.025</b>	<b>-0.025</b>	0.122	0	0.005	<b>-0.020</b>	-
<i>FV</i>	1	false	1	0.304	0.670	0	-	-	-	-	-	<b>-0.974</b>	0
<i>CSLAM</i>	1	false	1	0.312	0.239	0	-0.547	-0.557	0.620	0.010	-0.011	-0.558	<b>-0.070</b>
<i>CSLAM default</i>	5	true	2	0.320	-0.342	-	-0.524	-0.537	0.641	0.013	-0.011	-0.535	-

366 to match Table entries with discussion in the text. Important changes to TE errors are  
 367 marked with bold font in Table 1.

368 Various configurations are used and referred to in terms of the *COMPSET* (Com-  
 369 ponent Set) value used in CESM2.1. The *COMPSET F2000climo* configuration refers  
 370 to ‘real-world’ AMIP (Atmospheric Model Intercomparison Project) type simulations us-  
 371 ing perpetual year 2000 SST (Sea Surface Temperature) boundary conditions. The first 7  
 372 simulations in the table (those above the horizontal line) are such AMIP-type simulations  
 373 (*F2000climo*) with the first serving as a control for the 6 following variants. The remain-  
 374 ing 5 simulation descriptors (below the horizontal line in Table 1) list their *COMPSET* or  
 375 dynamical core settings.

- 376 • *TE consistent*: The TE consistent version uses *state update* physics-dynamics cou-  
 377 pling (*ftype* 1) described in section 3.1,
- 378 • ‘*dribbling*’ A: as *TE consistent* but with *dribbling* physics-dynamics coupling (*ftype*  
 379 0) (section 3.2),
- 380 • ‘*dribbling*’ B: as *TE consistent* but with *dribbling* combination physics-dynamics  
 381 coupling (*ftype* 2) (section 3.2),
- 382 • *vert limiter*: as *TE consistent* but using limiters in the vertical remapping of mo-  
 383 mentum (section 3.3),
- 384 • *smooth topo*: as *TE consistent* but using smoother topography (see section 3.4),
- 385 • *energy discr*: The version with energy discrepancy (but no physics-dynamics cou-  
 386 pling errors) described in section 3.5,
- 387 • *default*: as *energy discr* version but with *ftype*=2 which is the current default  
 388 CAM-SE (section 3.5),
- 389 • *QPC6*: A simplified aqua-planet setup based on the *TE consistent*, i.e. an aqua-  
 390 planet setup using CAM6 physics; an ocean covered planet in perpetual equinox,  
 391 with fixed, zonally symmetric sea surface temperatures [Neale and Hoskins, 2000;  
 392 Medeiros et al., 2016] (section 3.6),
- 393 • *FSH94*: Dry dynamical core configuration based on Held-Suarez forcing which re-  
 394 laxes temperature to a zonally symmetric equilibrium temperature profile and sim-  
 395 ple linear drag at the lower boundary [Held and Suarez, 1994] (section 3.7).,
- 396 • *FV*: A configuration with the SE dynamical core replaced with the finite-volume  
 397 core (section 3.8), and
- 398 • *CSLAM*: The quasi equal-area physics grid configuration of CAM-SE based on the  
 399 TE consistent setup (section 3.9)
- 400 • *CSLAM default*: Same as *CSLAM* configuration but with *ftype*=2 and all forms of  
 401 water thermodynamically active in the dynamical core.

### 408 3.1 *TE consistent: state-update* physics-dynamics coupling (*ftype*=1) and no TE 409 formula discrepancy

410 This configuration is the most energetically consistent in that the physical parame-  
 411 terizations and the continuous equations of motion on which the dynamical core is based,  
 412 conserve the same TE (defined in equation (8)); and there are no spurious sources/sinks in  
 413 physics-dynamics coupling. Energetic consistency in dynamics and physics is obtained  
 414 by setting  $c_p^{(\ell)} \equiv c_p^d$  and  $\mathcal{L}_{all} = \{‘d’, ‘wv’\}$  in the dynamical core equations of mo-  
 415 tion and TE computations. Associated namelist changes resulting in this configuration are  
 416 `lcp_moist = .false., se_qsize_condensate_loading = 1, and ftype = 1.`

417 The TE consistent configuration in AMIP-type simulation (*F2000climo*) is used to  
 418 compute baseline TE tendencies which will be used to compare with other model con-  
 419 figurations. First we establish how long an average is needed to get robust TE tendency  
 420 estimates. Figure 2 shows  $\partial\hat{E}$  for various aspects of CAM-SE as a function of time. The  
 421 simulation length is 5 years and monthly average values are used for the analysis. First

422 consider the left plot. The TE tendency from parameterizations ( $\partial\widehat{E}_{phys}^{(param)}$ ) show significant variability with an amplitude of approximately  $2.5W/m^2$ . As noted above this term  
 423 does not figure in the spurious TE budget. The net source/sink provides an equal and opposite term to balance it. That said, the variability is reflected onto the TE tendency due  
 424 to pressure work  $\partial\widehat{E}_{phys}^{(pwork)} \approx 0.32 \pm 0.08W/m^2$ . On the scale used in the left-hand plot  
 425 the TE tendency of the adiabatic dynamical core  $\partial\widehat{E}_{dyn}^{(adiab)}$  does not seem to be affected  
 426 by  $\partial\widehat{E}_{phys}^{(param)}$  or  $\partial\widehat{E}_{phys}^{(pwork)}$  in terms of variability, and remains stable at approximately  
 427  $-0.6W/m^2 \pm 0.02W/m^2$ . The TE fixer, in this model configuration, fixes  $\partial\widehat{E}_{dyn}^{(adiab)}$  and  
 428  $\partial\widehat{E}_{phys}^{(pwork)}$ . Since the TE imbalance in the adiabatic dynamics remains approximately constant  
 429 and the TE tendency associated with pressure work has variability, the TE tendency from the  $\partial\widehat{E}_{phys}^{(efix)}$  has variability;  $\partial\widehat{E}_{phys}^{(efix)} \approx 0.30 \pm 0.08W/m^2$ . As a consistency check  
 430  $-\partial\widehat{E}_{dyn}^{(adiab)} - \partial\widehat{E}_{phys}^{(pwork)}$  is plotted with asterisk's and they coincide (as expected) with  
 431  $\partial\widehat{E}_{phys}^{(efix)}$  fulfilling (22).

435 The right-hand plot in Figure 2 shows a breakdown of the dynamical core TE tendencies.  
 436 The majority of the TE errors are due to hyperviscosity on temperature and pressure,  
 437  $\partial\widehat{E}_{dyn}^{(hvis)} \approx -0.61 \pm 0.01W/m^2$ . The diffusion of momentum is added back as  
 438 frictional heating and is therefore not part of  $\partial\widehat{E}_{dyn}^{(hvis)}$ . The frictional heating is a significant  
 439 term in the TE tendency budget  $\partial\widehat{E}_{dyn}^{(fheat)} \approx 0.56 \pm 0.02W/m^2$  and exhibits  
 440 some variability but with a rather small amplitude. The remaining TE error in the floating  
 441 Lagrangian dynamics is inviscid dissipation and time-truncation errors  $\partial\widehat{E}_{dyn}^{(res)} =$   
 442  $\partial\widehat{E}_{dyn}^{(2D)} - \partial\widehat{E}_{dyn}^{(hvis)} \approx 0.007W/m^2$ . The TE tendency from vertical remapping is ap-  
 443 proximately  $\partial\widehat{E}_{dyn}^{(remap)} \approx -0.01W/m^2$ . To within  $\sim 0.02W/m^2$  the dynamical core TE  
 444 tendency terms can be computed from just one month average TE integrals. The TE ten-  
 445 dencies computed in physics, excluding  $\partial\widehat{E}_{phys}^{(param)}$ , exhibit more variability and are only  
 446 accurate to  $\sim 0.1W/m^2$  after a one month average.

447 While it is advantageous to use *state-update* physics-dynamics coupling algorithm  
 448 (`ftype=1`) in terms of having no spurious TE tendency from coupling,  $\partial\widehat{E}^{(pdc)} = 0$ ,  
 449 it does result in spurious gravity waves in the simulations [see, e.g., Figure 5 in *Gross*  
 450 *et al.*, 2018]. Figure 3a shows a 1 year average of  $|\frac{d\mathbf{p}_s}{dt}|$ , a measure of high frequency  
 451 gravity wave noise. It clearly exhibits unphysical oscillations coinciding with element  
 452 boundaries. Details of the spectral-element method, its coupling to physics and associ-  
 453 ated noise issues are discussed in detail in *Herrington et al.* [2018]. The noise in the sol-  
 454 tions is even visible in the 500hPa pressure velocity annual average (Figure 4a). This  
 455 issue can be alleviated by using a shorter physics time-step so that the physics increments  
 456 are smaller (not shown). Climate modelers have historically not pursued a shorter physics  
 457 time-step in production configurations as climate parameterizations are computationally  
 458 expensive and there is a large sensitivity to physics time-steps in the simulated climate  
 459 [e.g. *Williamson and Olson*, 2003; *Wan et al.*, 2015].

### 460 3.2 ‘dribbling’ A/B: Non-TE conservative physics-dynamics coupling (`ftype=0, 2`)

#### 461 3.2.1 Element boundary noise

462 When switching to *dribbling* physics-dynamics coupling algorithm (`ftype=0`) in  
 463 which the tendencies from physics are added throughout the dynamics (in this case twice  
 464 per physics time-step) then the noise issues described in previous section disappear (Figure  
 465 3b and 4b). That said, there is a significant issue with this approach; the tracer mass bud-  
 466 gets may not be closed. How this comes about is illustrated in Figure 5 and explained in  
 467 the next paragraph.

468 The orange curve on Figure 5a, b, d, and e is the initial state of, e.g., cloud liq-  
 469 uid mixing ratio as a function of location, e.g., longitude. Cloud liquid is zero outside

of clouds and hence provides a good example for the purpose of this illustration. The light blue arrows show the increments (in terms of length of arrow) computed by the parameterizations based on the initial state and scaled for the partial update with *dribbling* (`ftype=0`). With *state-update* (`ftype=1`) the increments from physics are added to the dynamical core state (dotted line on 5b) before the dynamical core advances the solution in time. The parameterizations are designed to not drive the mixing ratios negative so the state-update in dynamics will not generate negatives (or overshoots). Then the dynamical core advects the distribution (solid curve on Figure 5c). With *dribbling* (`ftype=0`) the physics increments are split into equal chunks (in this illustration two; blue errors on Figure 5d). Half of the physics increments are added to the initial state (dotted line on Figure 5e) and then dynamics advects the distribution half of the total dynamical core steps (dashed line on Figure 5e). Then the other half of the physics increments are applied (in the same location as they were computed by physics). Now after the previous/first advection step the cloud liquid distribution has moved and the mixing ratio may be zero (or less than the increment prescribed by physics) where the physics forcing is applied (e.g., left side of dashed curve). Hence the physics increment is driving the mixing ratios negative in those locations. Thereafter the distribution is advected (solid curve on Figure 5f). In CAM the increments added in the dynamical core are limited so that they drive the mixing to zero (but not negative) if this problem occurs. This leads to a net source of mass compared to the mass change that the parameterizations prescribe (see Figure 6). Although the average source of mass is small each time-step it always has the same sign (i.e. it is a bias) and therefore accumulates. *Zhang et al.* [2017] estimated that this spurious source of mass is equivalent to  $\sim 10\text{cm}$  sea-level rise per decade in coupled climate simulation experiments.

The majority of the noise with *state-update* (`ftype=1`) physics-dynamics coupling method comes from momentum sources/sinks and heating/cooling. A way to alleviate noise problems and, at the same time, close the tracer mass budgets (in physics-dynamics coupling) is to use *state-update* (`ftype=1`) coupling for tracers and *dribbling* (`ftype=0`) coupling for momentum and temperature (referred to as *combination*, `ftype=2`). Figure 3c shows the noise diagnostic  $|\frac{dp_s}{dt}|$  for *combination* (`ftype=2`) coupling. Figure 3c looks very similar to Figure 3b but there is some noise near element boundaries. That said, in terms of vertical pressure velocities *combination* (`ftype=2`) and *dribbling* (`ftype=0`) climates are similar in terms of the level of noise (Figure 4b and 4c). The element noise in CAM-SE with *combination* (`ftype=2`) seen in both  $|\frac{dp_s}{dt}|$  and 500hPa pressure velocity can be ‘removed’ by using CAM-SE-CSLAM (Figure 3d) which uses a quasi equal-area physics grid and CSLAM [Conservative Semi-Lagrangian Multi-tracer; *Lauritzen et al.*, 2010] consistently coupled to the SE method [*Lauritzen et al.*, 2017]. The noise patterns in vertical velocity off the western coast of South America are present in all CAM-SE simulations (and hence not related to physics-dynamics coupling algorithm) are also ‘removed’ by using CAM-SE-CSLAM [*Herrington et al.*, 2018].

### 3.2.2 Spurious TE tendencies from physics-dynamics coupling

When using the same TE formula in the dynamical core and physics the spurious TE tendency from physics-dynamics coupling can be assessed. Since the pressure fields evolve during *dribbling* of physics forcing, the TE increments from the forcing change. For *dribbling* (`ftype=0`) and *combination* (`ftype=2`) this tendency is  $\partial \widehat{E}^{(pdc)} = -0.05\text{W/m}^2$  and thus rather small compared to the viscosity TE dissipation rates. Since  $\partial \widehat{E}^{(pdc)}$  are the same (to the second digit) for *dribbling* (`ftype=0`) and *combination* (`ftype=2`) it is the momentum and temperature *dribbling* errors that dominate  $\partial \widehat{E}^{(pdc)}$ .

## 3.3 *vert limiter*: Limiters on vertical remapping of momentum

CAM-SE uses a floating Lagrangian vertical coordinate [*Starr*, 1945; *Lin*, 2004] which requires the remapping of the atmospheric state from floating levels back to refer-

ence levels to maintain computational stability and to provide state data consistent with the physics formulation. The mapping algorithm is based on the mass conservative PPM (Piecewise Parabolic Method) with options for shape-preserving limiters. In CAM-SE momentum components and internal energy are used as the variables mapped in the vertical [Lauritzen *et al.*, 2018] and, contrary to earlier versions of CAM-SE, there is no limiter on the remapping of wind components. If the shape-preserving limiter is used for momentum mapping then the TE dissipation increases by over an order of magnitude from  $\sim 0.01W/m^2$  to  $\sim 0.2W/m^2$  (Table 1).

### 3.4 smooth topo: Smoother topography

Topography for CAM is generated using a new version of the software/algorithm described in Lauritzen *et al.* [2015] that is available at <https://github.com/NCAR/Topo>. The updates to the software includes smoothing algorithms and the computation of sub-grid-scale orientation of topography.

The default topography in CAM-SE uses the same amount of topography smoothing as CAM-FV (distance weighted smoother applied to the raw topography on  $\sim 3\text{km}$  cubed-sphere grid with a smoothing radius of 180km referred to as C60). When the topography is smoother (in this case using C92 smoothing, i.e. smoothing radius of approximately 276km) the hyperviscosity operators are less active leading to reduced TE errors, i.e.  $\partial\widehat{E}_{dyn}^{(hvis)}$  is reduced in half from approximately  $-0.6W/m^2$  to  $-0.3W/m^2$ . The vertical remapping TE error, however, remains approximately the same. Since the pressure work is approximately  $0.3W/m^2$  it almost exactly compensates for the TE tendency from the dynamical core  $\partial\widehat{E}_{dyn}^{(adiab)}$ . Hence if one would only diagnose the TE tendency from the energy fixer one could mistakenly conclude that the model universally conserves TE when, in fact, there are compensating TE errors in the system. These compensating errors can only be diagnosed through a careful breakdown of the total TE tendencies.

### 3.5 default: TE formula discrepancy errors

To assess the TE errors due to the discrepancy in the energy formula used by dynamics and physics, a simulation using *state-updating* (*ftype*=1, no ‘dribbling’ errors) and thermodynamically active condensates in the dynamical core (*qsize\_condensate\_loading* = 5) and consistent/accurate associated heat capacities  $c_p^{(\ell)}$  (namelist *lcp\_moist=.true.*) has been performed. In this setup the continuous equations of motion in the dynamical core conserve an energy different from physics, and the energy fixer will restore the ‘physics’ version of energy. Despite the dynamical core now using a more comprehensive formula for energy, the TE dissipation terms in the dynamical core are roughly the same as in the energy consistent versions of the model. Using (25) we can assess the TE energy discrepancy errors which result in  $\sim 0.59W/m^2$ . Taylor [2011] found a similar result just from using the more comprehensive formula for heat capacity (based on dry air and water vapor) and not including thermodynamically active condensates. As noted before this formulation inconsistency is due to the evolutionary nature of CAM development and it is the intention to remove this inconsistency in future versions of the model.

The default version of CAM-SE uses this configuration but with *combination* (*ftype*=2) which has similar TE characteristics (see Table 1). That said, the physics-dynamics coupling error from *dribbling* momentum and temperature tendencies and the energy discrepancy errors can not be separated in this configuration:

$$\partial\widehat{E}^{(pdc)} + \partial\widehat{E}^{(discr)} = 0.546W/m^2, \quad (26)$$

using (22). With *state-updating* (*ftype*=1) (i.e.  $\partial\widehat{E}^{(pdc)} = 0$ ) the energy discrepancy error was  $0.594W/m^2$  and in the energy consistent setup (i.e.  $\partial\widehat{E}^{(discr)} = 0$ ) but using *dribbling* (*ftype*=2) we got  $\partial\widehat{E}^{(pdc)} = 0.484W/m^2$ . So if the physics-dynamics coupling errors and energy discrepancy errors in the different configurations would be additive, one would

569 have expected  $\partial\widehat{E}^{(pdc)} + \partial\widehat{E}^{(discr)}$  to be over  $1W/m^2$  which is clearly not the case (26).  
 570 Again, it must be concluded that there are canceling errors in the system.

### 571 3.6 QPC6: Simplified surface

572 By running the model in aqua-planet configuration one can assess the effect of sim-  
 573 plifying the surface boundary condition. In particular, without topography forcing the dy-  
 574 namical core is not challenged with respect to stationary near-grid-scale forcing. The TE  
 575 tendency with respect to pressure work remains the same  $\partial\widehat{E}_{phys}^{(pwork)}$  as the AMIP-type  
 576 simulations, however, the adiabatic dynamical core TE tendency reduces to  $\partial\widehat{E}_{dyn}^{(adiab)} =$   
 577  $-0.14W/m^2$  (approximately a factor 4 reduction). Most of that reduction is due to vis-  
 578 cosity  $\partial\widehat{E}_{dyn}^{(hvis)} = -0.13W/m^2$ . The frictional heating is roughly the same as AMIP  
 579  $\partial\widehat{E}_{dyn}^{(fheat)} = 0.48W/m^2$  as is the vertical remapping  $\partial\widehat{E}_{dyn}^{(remap)} = -0.01W/m^2$ . To eval-  
 580 uate the dynamical cores diffusion of TE it is therefore important to asses the model in  
 581 a configuration with topography as the wave dynamics generated by topography leads to  
 582 more active diffusion operators.

### 583 3.7 FHS94: Simplified physics (no moisture)

584 Simplifying the setup even further by replacing the parameterizations with relax-  
 585 ation towards a zonally symmetric temperature profile and simple boundary layer friction  
 586 (Held-Suarez forcing) as well as excluding moisture, the TE errors in the dynamical core  
 587 decreases even further to  $\sim 0.002W/m^2$  since there is no small scale forcing. Small scales  
 588 are only created by the nonlinear dynamics and the physics works to damp them. Hyper-  
 589 viscosity is less active leading to significant reductions compared to aqua-planet and ‘real-  
 590 world’ simulation results. The TE diffusion in vertical remapping reduces by an order of  
 591 magnitude compared to the aqua-planet simulations ( $\sim 0.0005W/m^2$ ). This further em-  
 592 phasizes that TE diffusion assessment in a simplified setup is not necessarily telling for  
 593 the dynamical cores performance with moist physics and topography that challenge the  
 594 dynamical core in terms of strong grid-scale forcing.

### 595 3.8 FV: Changing dynamical core to Finite-Volume (FV)

596 As a comparison the TE error characteristics of the CAM-FV dynamical core are  
 597 assessed. Although the TE diagnostics have not been implemented in the CAM-FV dy-  
 598 namical core, the TE diagnostics in CAM physics are independent of dynamical core  
 599 and can therefore be activated with CAM-FV. The CAM-FV dynamical core uses *state-*  
 600 *update* physics-dynamics coupling (`fptype=1`) ( $\partial\widehat{E}^{(pdc)} = 0$ ) and the same TE definition  
 601 as CAM physics ( $\partial\widehat{E}^{(discr)} = 0$ ). Hence (23) can be used to compute the TE errors of  
 602 the CAM-FV dynamical core,  $\partial\widehat{E}_{dyn}^{(adiab)} \approx -1W/m^2$ . As we do not have the break-down  
 603 of  $\partial\widehat{E}_{dyn}^{(adiab)}$  it can not be determined how much of the TE errors are due to the vertical  
 604 remapping. Furthermore, CAM-FV contains intrinsic dissipation operators (limiters in the  
 605 flux operators) making it difficult to assess TE sources/sinks due to dissipation. Note that  
 606 the pressure work even with a change of dynamical core remains approximately the same  
 607 as the CAM-SE configurations.

### 608 3.9 CSLAM: Quasi equal-area physics grid

609 This configuration was discussed in the context of element noise in section 3.2.1.  
 610 By averaging the dynamics state of an equal-partitioning (in central angle cubed-sphere  
 611 coordinates) of the elements, the element-boundary noise found in CAM-SE can be re-  
 612 moved. Lauritzen *et al.* [2018] argue that this way of computing the state for the physics  
 613 is more consistent with physics in terms of providing a cell-averaged state instead of ir-  
 614 regularly spaced point (quadrature) values. In order to achieve a closed mass-budget, this

615 configuration uses CSLAM for tracer transport rather than SE transport. That said, the  
 616 physics columns no longer coincide with the quadrature grid and there are TE errors asso-  
 617 ciated with mapping state and tendencies between the two grids.

618 In this configuration the energy diagnostics computed in the dynamical core are  
 619 computed on the quadrature grid and the energy diagnostics computed in physics are on  
 620 the physics grid. If the TE consistent configuration is used (`ftype=1, qsize_condensate_loading=1,`  
 621 `lcp_moist=.false.`) then the physics-dynamical coupling errors,  $\widehat{E}^{(pdc)}$  computed with  
 622 (20), are entirely due to mapping state from quadrature grid to physics grid and map-  
 623 ping tendencies back the quadrature grid from the physics grid. The results is  $\widehat{E}^{(pdc)} =$   
 624  $-0.07W/m^2$  which is a rather small error compared to other terms in the TE budget.

625 Due to similar noise problems with CAM-SE-CSLAM when using `ftype=1` that  
 626 were observed in CAM-SE (Figure 3 and 4), the default version of CAM-SE-CSLAM uses  
 627 `ftype=2`. Again physics-dynamics coupling errors and TE discrepancy errors can not be  
 628 separated;  $\partial\widehat{E}^{(pdc)} + \partial\widehat{E}^{(discr)} = 0.557W/m^2$ .

## 631 4 Conclusions

632 A detailed total energy (TE) error analysis of the Community Atmosphere Model  
 633 (CAM) using version 6 physics (included in the CESM2.1 release) running at approxi-  
 634 mately  $1^\circ$  horizontal resolution has been presented. In the global climate model there can  
 635 be many spurious contributions to the TE budget. These errors can be divided into four  
 636 categories: physical parameterizations, adiabatic dynamical core, the coupling between  
 637 physics and dynamics, and TE definition discrepancies between dynamics and physics.  
 638 The latter is not by design but through the evolutionary nature of model development. By  
 639 capturing the atmospheric state at various locations in the model algorithm, a detailed  
 640 budget of TE errors can be constructed. The net spurious TE energy errors are com-  
 641 pensated with a global energy fixer (providing a global uniform temperature increment) every  
 642 physics time-step.

643 In CAM physics the parameterizations have, by design, a closed energy budget (change  
 644 in TE is balanced by fluxes in/out the top and bottom of physics columns) if it is assumed  
 645 that pressure is not modified. However, the pressure changes due to fluxes of mass (e.g.,  
 646 water vapor) in/out of the column which changes energy (referred to as pressure work).  
 647 The pressure work with the full moist physics configuration is very stable across differ-  
 648 ent configurations at  $\sim 0.3W/m^2$ . The TE errors in the spectral element (SE) dynamical  
 649 core varies across configurations. Aspects that influence TE is the presence of topogra-  
 650 phy, the amount of topography smoothing and moist physics. By smoothing topography  
 651 more the TE error is cut in half from  $\sim -0.6W/m^2$  to  $\sim -0.3W/m^2$ ; and reduces by a  
 652 factor of five ( $\sim -0.1W/m^2$ ) if no topography is present at all (aqua-planet configuration).  
 653 Moist physics forcing also contributes significantly to the TE budget. For example, in the  
 654 dry Held-Suarez setup TE dissipation of the SE dynamical core reduces to  $-0.03W/m^2$ .  
 655 Topography and moist physics force the dynamical core at the grid scale and hence the  
 656 viscosity operators are more active. Consistent with this statement is that the changes in  
 657 TE discussed so far are almost entirely due to the viscosity operator TE dissipation. For  
 658 CAM-SE the spurious TE dissipation in the adiabatic dynamical core is  $\sim -0.6W/m^2$  in  
 659 ‘real-world’ configurations. For comparison, CAM-FV’s spurious TE change due to the  
 660 adiabatic dynamical core is  $\sim -1W/m^2$ .

661 By further breaking down the TE dissipation in the SE dynamical core it is ob-  
 662 served the vertical remapping accounts for only  $\sim -0.01W/m^2$ . That said, if the shape-  
 663 preserving limiters in the vertical remapping are invoked the TE dissipation increases 20-  
 664 fold to  $\sim -0.2W/m^2$ . In CAM-SE the kinetic energy dissipation is added as heating in  
 665 the thermodynamic equation (also referred to as frictional heating). The frictional heat-  
 666 ing remains very stable across configurations that include moisture ( $\sim 0.5W/m^2$ ) and re-

duces drastically for dry atmosphere setups (factor 4 reduction to ( $\sim 0.12W/m^2$ )). Hence this term is an important term in the TE budget. The TE budget for the dynamical core is dominated by TE change due to hyperviscosity; TE errors due to time-truncation and frictionless equations of motion are negligible. Errors associated with physics-dynamics coupling (if applicable) are approximately  $0.5W/m^2$ . Due to the evolutionary nature of model development the SE dynamical core's continuous equation of motion conserve a more comprehensive TE compared to the physical parameterizations. This TE discrepancy leads to an approximately  $0.5W/m^2$  total energy source. Running physics on a different grid than the dynamical introduces TE mapping errors such as in CAM-SE-CSLAM (Conservative Semi-Lagrangian Multi-tracer transport scheme). These errors are, however, rather small  $-0.07W/m^2$ .

A purpose of this paper is to better understand the energy characteristics of CAM and to encourage modeling groups to perform similar analysis to better understand the total energy flow in the atmospheric component of Earth system models. As has been demonstrated in this paper there can easily be compensating errors in the system which can not be identified without a detailed TE analysis.

### Acknowledgments

The National Center for Atmospheric Research is sponsored by the National Science Foundation. Computing resources (doi:10.5065/D6RX99HX) were provided by the Climate Simulation Laboratory at NCAR's Computational and Information Systems Laboratory, sponsored by the National Science Foundation and other agencies. The data used to perform the energy analysis can be found at <https://github.com/PeterHjortLauritzen/2018-JAMES-energy>.

### References

- Boville, B. (2000), chap. Toward a complete model of the climate system in Numerical Modeling of the Global Atmosphere in the Climate System, pp. 419–442, Springer Netherlands.
- Computational and Information Systems Laboratory (2017), Cheyenne: HPE/SGI ICE XA System (Climate Simulation Laboratory), Boulder, CO: National Center for Atmospheric Research, doi:10.5065/D6RX99HX.
- Eldred, C., and D. Randall (2017), Total energy and potential enstrophy conserving schemes for the shallow water equations using hamiltonian methods – part 1: Derivation and properties, *Geosci. Model Dev.*, 10(2), 791–810, doi:10.5194/gmd-10-791-2017.
- Gross, M., H. Wan, P. J. Rasch, P. M. Caldwell, D. L. Williamson, D. Klocke, C. Jablonowski, D. R. Thatcher, N. Wood, M. Cullen, B. Beare, M. Willett, F. Lemarié, E. Blayo, S. Malardel, P. Termonia, A. Gassmann, P. H. Lauritzen, H. Johansen, C. M. Zarzycki, K. Sakaguchi, and R. Leung (2018), Physics-dynamics coupling in weather, climate and earth system models: Challenges and recent progress, *Mon. Wea. Rev.*, 146, 3505–3544, doi:10.1175/MWR-D-17-0345.1.
- Held, I. M., and M. J. Suarez (1994), A proposal for the intercomparison of the dynamical cores of atmospheric general circulation models, *Bull. Amer. Meteor. Soc.*, 75, 1825–1830.
- Herrington, A. R., P. H. Lauritzen, M. A. Taylor, S. Goldhaber, B. E. Eaton, K. A. Reed, and P. A. Ullrich (2018), Physics-dynamics coupling with element-based high-order Galerkin methods: quasi equal-area physics grid, *Mon. Wea. Rev.*
- Jablonowski, C., and D. L. Williamson (2011), chap. The Pros and Cons of Diffusion, Filters and Fixers in Atmospheric General Circulation Models, pp. 381–493, Springer Berlin Heidelberg, Berlin, Heidelberg, doi:10.1007/978-3-642-11640-7\_13.

- 716 Kasahara, A. (1974), Various vertical coordinate systems used for numerical weather pre-  
 717 diction, *Mon. Wea. Rev.*, 102(7), 509–522.
- 718 Lauritzen, P. H., R. D. Nair, and P. A. Ullrich (2010), A conservative semi-Lagrangian  
 719 multi-tracer transport scheme (CSLAM) on the cubed-sphere grid, *J. Comput. Phys.*,  
 720 229, 1401–1424, doi:10.1016/j.jcp.2009.10.036.
- 721 Lauritzen, P. H., J. T. Bacmeister, T. Dubos, S. Lebonnois, and M. A. Taylor (2014),  
 722 Held-Suarez simulations with the Community Atmosphere Model Spectral Element  
 723 (CAM-SE) dynamical core: A global axial angular momentum analysis using Eule-  
 724 rian and floating Lagrangian vertical coordinates, *J. Adv. Model. Earth Syst.*, 6, doi:  
 725 10.1002/2013MS000268.
- 726 Lauritzen, P. H., J. T. Bacmeister, P. F. Callaghan, and M. A. Taylor (2015), NCAR\_Topo  
 727 (v1.0): NCAR global model topography generation software for unstructured grids,  
 728 *Geosci. Model Dev.*, 8(12), 3975–3986, doi:10.5194/gmd-8-3975-2015.
- 729 Lauritzen, P. H., M. A. Taylor, J. Overfelt, P. A. Ullrich, R. D. Nair, S. Goldhaber, and  
 730 R. Kelly (2017), CAM-SE-CSLAM: Consistent coupling of a conservative semi-  
 731 lagrangian finite-volume method with spectral element dynamics, *Mon. Wea. Rev.*,  
 732 145(3), 833–855, doi:10.1175/MWR-D-16-0258.1.
- 733 Lauritzen, P. H., R. Nair, A. Herrington, P. Callaghan, S. Goldhaber, J. Dennis, J. T.  
 734 Bacmeister, B. Eaton, C. Zarzycki, M. A. Taylor, A. Gettelman, R. Neale, B. Dobbins,  
 735 K. Reed, and T. Dubos (2018), NCAR release of CAM-SE in CESM2.0: A reformu-  
 736 lation of the spectral-element dynamical core in dry-mass vertical coordinates with  
 737 comprehensive treatment of condensates and energy, *J. Adv. Model. Earth Syst.*, doi:  
 738 10.1029/2017MS001257.
- 739 Lin, S.-J. (2004), A 'vertically Lagrangian' finite-volume dynamical core for global mod-  
 740 els, *Mon. Wea. Rev.*, 132, 2293–2307.
- 741 McRae, A. T. T., and C. J. Cotter (2013), Energy- and enstrophy-conserving schemes for  
 742 the shallow-water equations, based on mimetic finite elements, *Quart. J. Roy. Meteor.  
 743 Soc.*, 140(684), 2223–2234, doi:10.1002/qj.2291.
- 744 Medeiros, B., D. L. Williamson, and J. G. Olson (2016), Reference aquaplanet climate in  
 745 the community atmosphere model, version 5, *J. Adv. Model. Earth Syst.*, 8(1), 406–424,  
 746 doi:10.1002/2015MS000593.
- 747 Neale, R. B., and B. J. Hoskins (2000), A standard test for AGCMs including their phys-  
 748 ical parametrizations: I: the proposal, *Atmos. Sci. Lett.*, 1(2), 101–107, doi:10.1006/asle.  
 749 2000.0022.
- 750 Neale, R. B., C.-C. Chen, A. Gettelman, P. H. Lauritzen, S. Park, D. L. Williamson, A. J.  
 751 Conley, R. Garcia, D. Kinnison, J.-F. Lamarque, D. Marsh, M. Mills, A. K. Smith,  
 752 S. Tilmes, F. Vitt, P. Cameron-Smith, W. D. Collins, M. J. Iacono, R. C. Easter, S. J.  
 753 Ghan, X. Liu, P. J. Rasch, and M. A. Taylor (2012), Description of the NCAR Commu-  
 754 nity Atmosphere Model (CAM 5.0), *NCAR Technical Note NCAR/TN-486+STR*, National  
 755 Center of Atmospheric Research.
- 756 Skamarock, W. C., J. B. Klemp, M. G. Duda, L. Fowler, S.-H. Park, and T. D. Ringler  
 757 (2012), A multi-scale nonhydrostatic atmospheric model using centroidal Voronoi tes-  
 758 selations and C-grid staggering, *Mon. Wea. Rev.*, 240, 3090–3105, doi:doi:10.1175/  
 759 MWR-D-11-00215.1.
- 760 Starr, V. P. (1945), A quasi-Lagrangian system of hydrodynamical equations., *J. Atmos.  
 761 Sci.*, 2, 227–237.
- 762 Taylor, M. A. (2011), Conservation of mass and energy for the moist atmospheric prim-  
 763 itive equations on unstructured grids, in: P.H. Lauritzen, R.D. Nair, C. Jablonowski,  
 764 M. Taylor (Eds.), Numerical techniques for global atmospheric models, *Lecture Notes  
 765 in Computational Science and Engineering*, Springer, 2010, *in press.*, 80, 357–380, doi:  
 766 10.1007/978-3-642-11640-7\_12.
- 767 Thuburn, J. (2008), Some conservation issues for the dynamical cores of NWP and cli-  
 768 mate models, *J. Comput. Phys.*, 227, 3715–3730.

- Trenberth, K. E., and J. T. Fasullo (2018), Applications of an updated atmospheric energetics formulation, *J. Climate*, 31(16), 6263–6279, doi:10.1175/JCLI-D-17-0838.1.
- Wan, H., P. J. Rasch, M. A. Taylor, and C. Jablonowski (2015), Short-term time step convergence in a climate model, *J. Adv. Model. Earth Syst.*, 7(1), 215–225, doi:10.1002/2014MS000368.
- Williamson, D. L. (2002), Time-split versus process-split coupling of parameterizations and dynamical core, *Mon. Wea. Rev.*, 130, 2024–2041.
- Williamson, D. L., and J. G. Olson (2003), Dependence of aqua-planet simulations on time step, *Q. J. R. Meteorol. Soc.*, 129(591), 2049–2064.
- Williamson, D. L., J. G. Olson, C. Hannay, T. Toniazzo, M. Taylor, and V. Yudin (2015), Energy considerations in the community atmosphere model (cam), *J. Adv. Model. Earth Syst.*, 7(3), 1178–1188, doi:10.1002/2015MS000448.
- Zhang, K., P. J. Rasch, M. A. Taylor, H. Wan, L.-Y. R. Leung, P.-L. Ma, J.-C. Golaz, J. Wolfe, W. Lin, B. Singh, S. Burrows, J.-H. Yoon, H. Wang, Y. Qian, Q. Tang, P. Caldwell, and S. Xie (2017), Impact of numerical choices on water conservation in the e3sm atmosphere model version 1 (eam v1), *Geoscientific Model Development Discussions*, 2017, 1–26, doi:10.5194/gmd-2017-293.

```

do nt=1,ntotal

PARAMETERIZATIONS:
Last dynamics state received from dynamics
output 'pBF'
efix Energy fixer
output 'pBP'
phys param Physics updates the state and state saved for energy fixer
output 'pAP'
pwork Pressure work (dry mass correction)
output 'pAM'
Physics tendency (forcing) passed to dynamics

DYNAMICAL CORE
output 'dED'
do ns=1,nsplit
output 'dAF'

phys
START PHYSICS-DYNAMICS COUPLING
Update dynamics state with (1/nsplit) of physics tendency (ftype=2)
if (ns=1) Update dynamics state with entire physics tendency (ftype=1)
DONE PHYSICS-DYNAMICS COUPLING

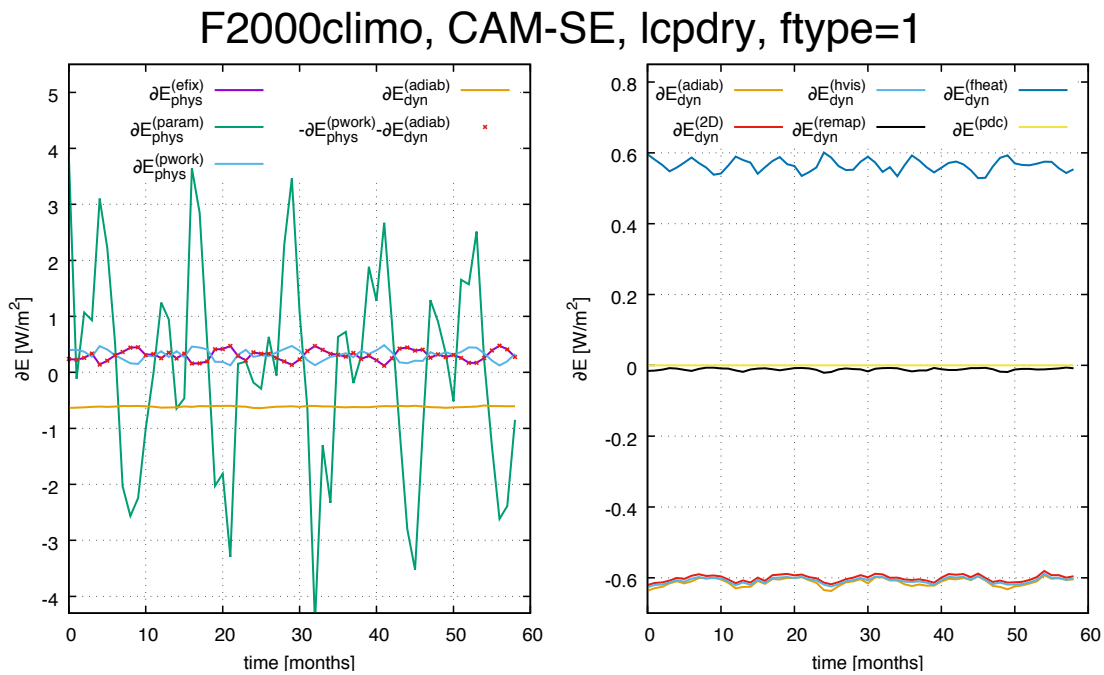
output 'dB'D'

adiab
2D
hvis
do nr=1,rsplit
Advance the adiabatic frictionless equations of motion
in floating Lagrangian layer
do ns=1,hypervis_subcycle
output 'dBH'
Apply hyperviscosity operators
output 'dCH'
fheat Add frictional heating to temperature
output 'dAH'
end do (ns=1,hypervis_subcycle)
end do (nr=1,rsplit)
output 'dAD'
remap
Vertical remapping from floating Lagrangian levels to Eulerian levels
output 'dAR'
end do (ns=1,nsplit)
Dynamics state saved for next model time step and passed to physics
output 'dB'F'

end do (nt=1,ntotal)

```

253 **Figure 1.** Pseudo-code for CAM-SE showing the order in which relevant physics updates are performed as  
254 well as dynamical core steps and associated loops. In green font locations where the state is captured and out-  
255 put is shown together with its 3 character identifier. The outer most loop (1, *ntotal*) advances the entire model  
256  $\Delta t_{phys}$  seconds (in this case 1800s). The dynamical core loops are as follows: the outer loop is the vertical  
257 remapping loop (1, *nsplit*) with associated time-step  $\Delta t_{phys}/nsplit$ . For stability the temporal advance-  
258 ment of the equations of motion in the Lagrangian layer needs to be sub-cycled *rsplit* times. Within the  
259 *rsplit*-loop the hyperviscosity time-stepping is sub-cycled *hypervis\_subcycle* times (again for stability).  
For more details on the time-stepping in CAM-SE see Lauritzen *et al.* [2018].



402 **Figure 2.** Monthly averaged TE tendencies as a function of time for various aspects of the TE consistent  
 403 configuration of CAM-SE run in AMIP-type configuration with perpetual year 2000 SSTs. Left Figure shows  
 404  $\partial \widehat{E}$  TE tendencies in physics and, for comparison, TE tendency for the adiabatic dynamical core. The right  
 405 plot shows the break-down of  $\partial \widehat{E}$  for the dynamical core. These plots show that the energy tendency from the  
 406 dynamical core is quite constant (to within  $\sim 0.02 W/m^2$  or less) so only one month simulations is adequate to  
 407 assess energy diagnostics for the dynamical core. For more details see Section 3.1.

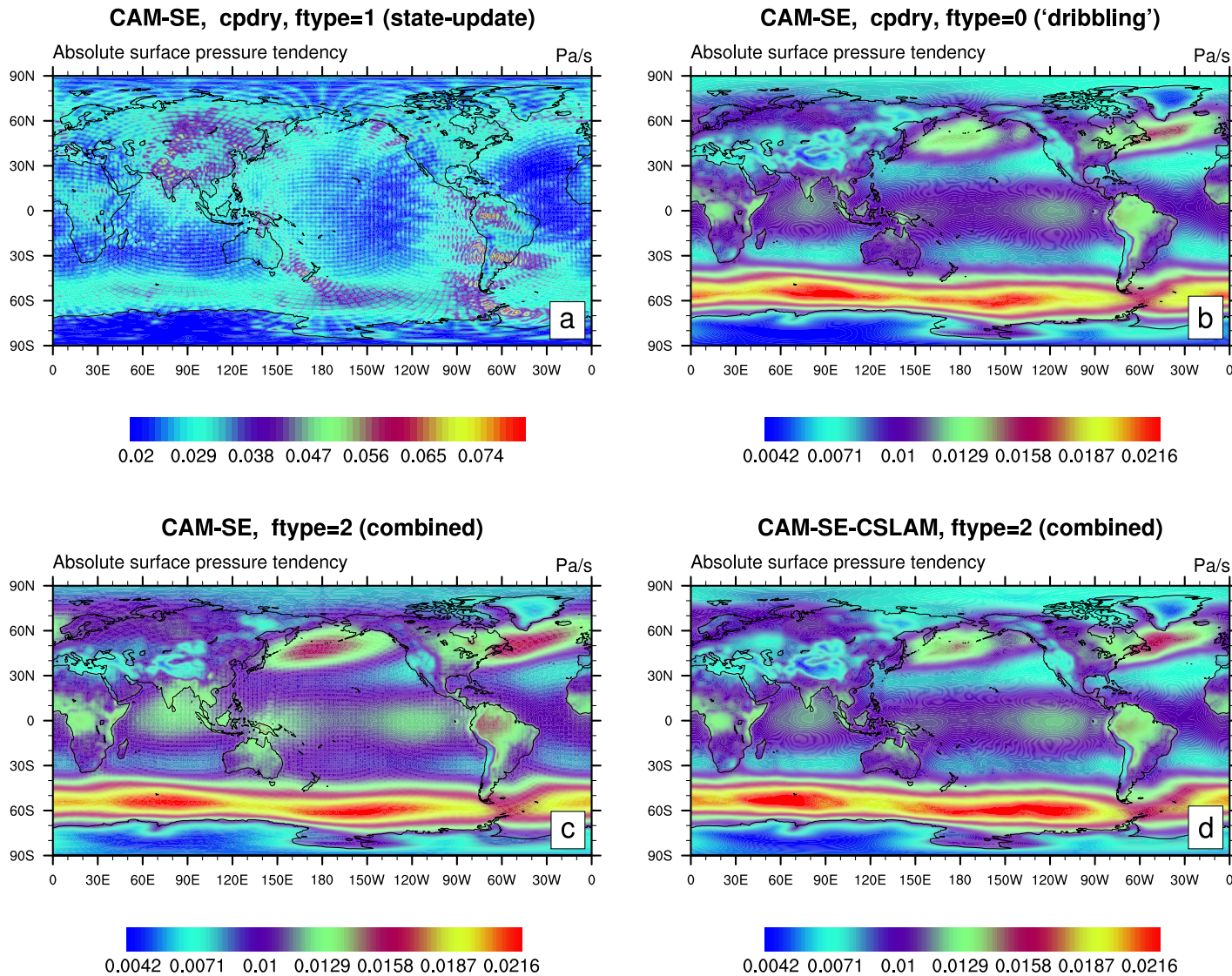


**Figure 3.** One year average of the absolute surface pressure tendency for (a) the TE consistent configuration, (b) ‘dribbling’ physics-dynamics coupling, (c) `ftype=2` physics-dynamics coupling and (d) CSLAM version of CAM-SE, respectively. (a) has a closed physics-dynamics coupling budget but spurious noise, (b) has no spurious noise but the mass-budget in physics-dynamics coupling is not closed (see Figure 6), (c) has a closed mass budget in physics-dynamics coupling but some spurious noise at element boundaries which is eliminated when using CAM-SE-CSLAM (d). Note, the smallest value in panel (a) is the largest in panels (b), (c) and (d).

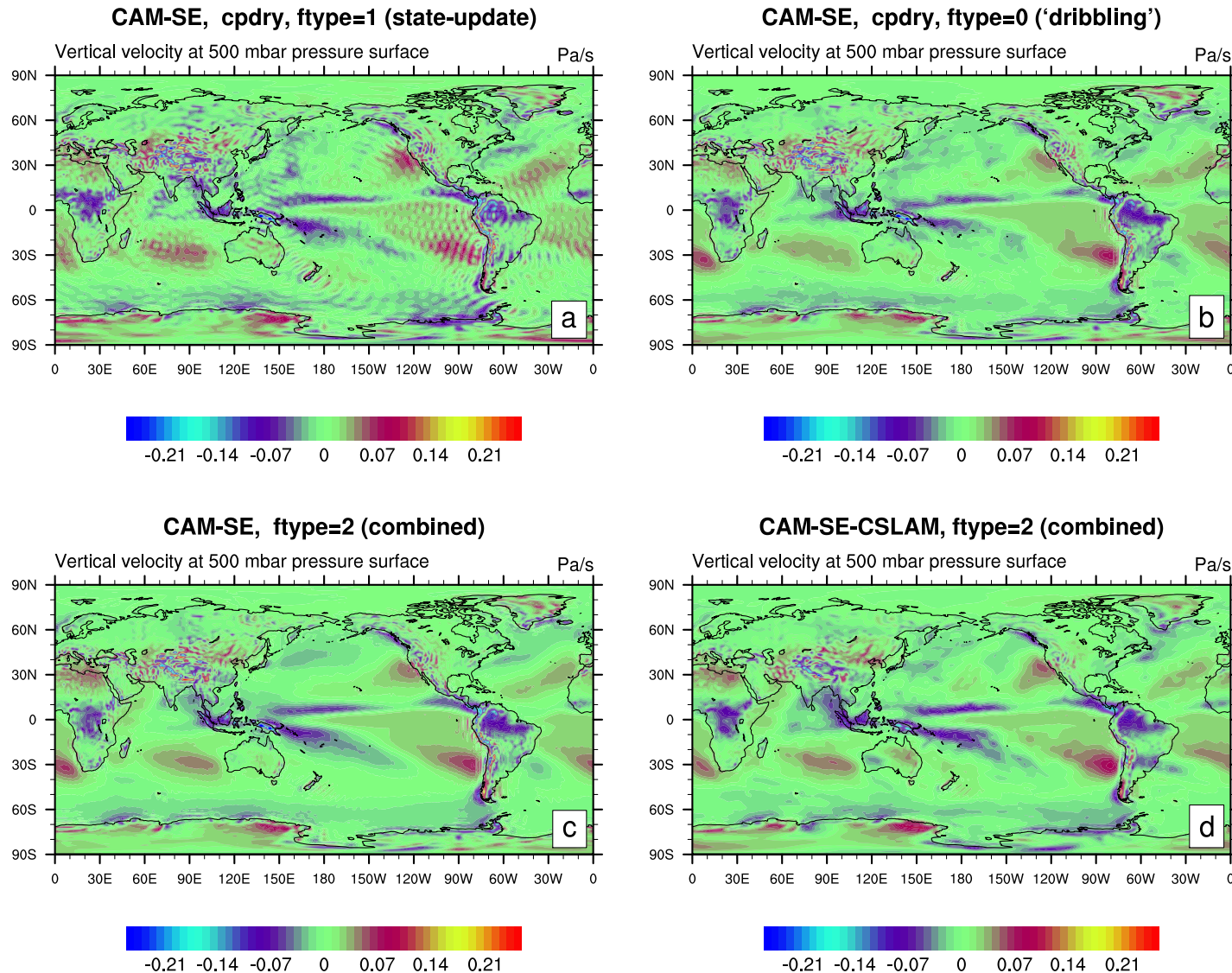


**Figure 4.** Same as Figure 3 but for 500hPa vertical pressure velocity. Note the ringing patterns off the West coast of South America and around the Himalayas in CAM-SE (a-c) that are eliminated with CAM-SE-CSLAM (d) that makes use of a quasi equal-area physics grid.

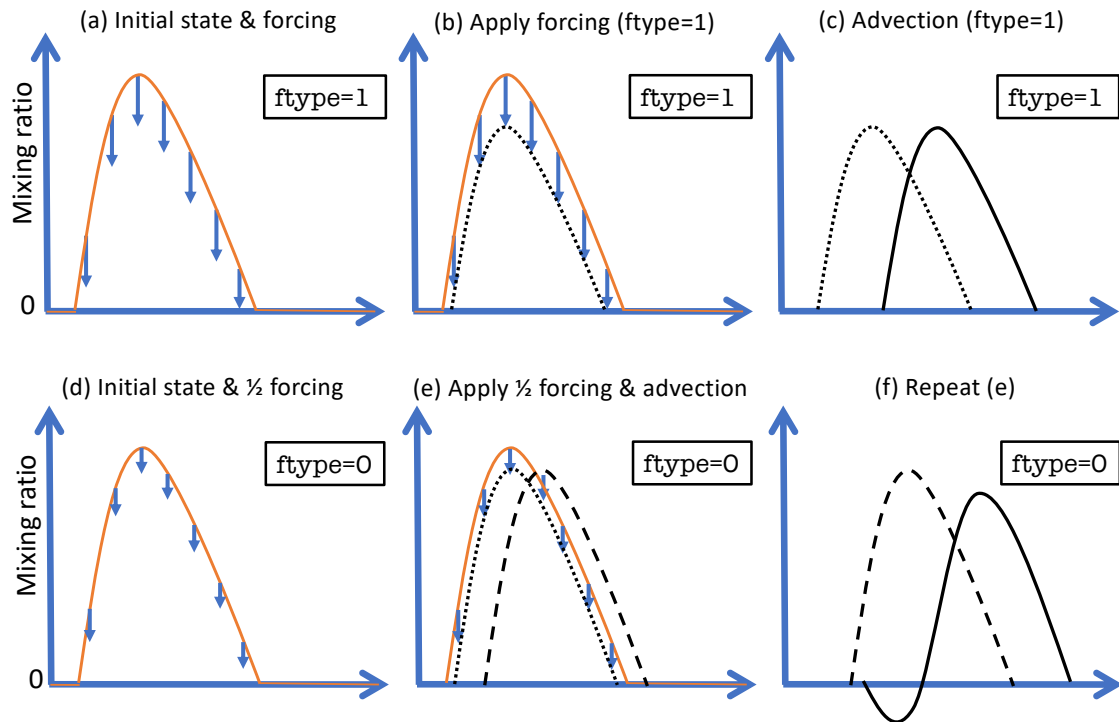


**Figure 5.** A schematic of state-update ( $\text{ftype}=1$ ; row 1) and ‘dribbling’ ( $\text{ftype}=0$ ; row 2) physics-dynamics coupling algorithms. See Section 3.2 for details.

## F2000climo, CAM-SE, cpdry, ftype=0 ('dribbling')

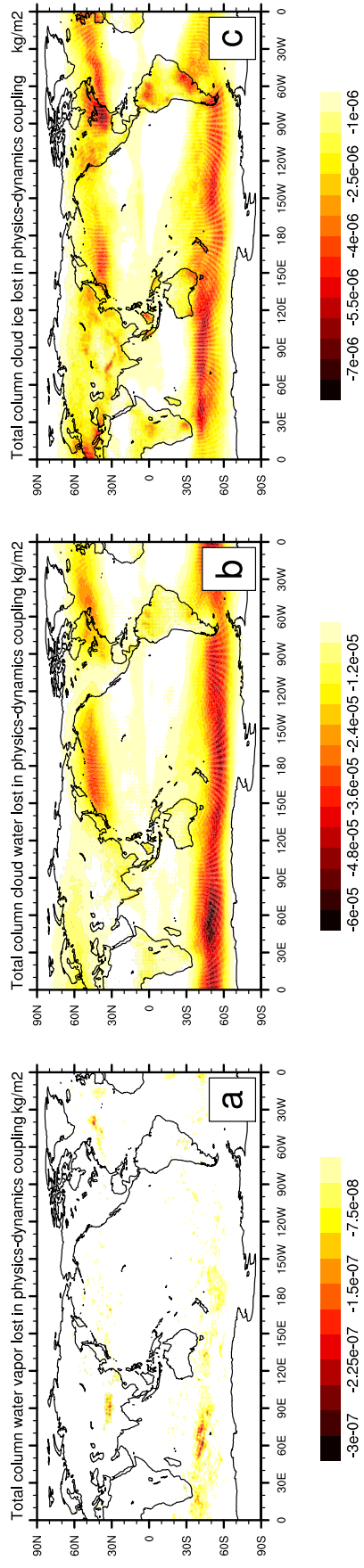


**Figure 6.** One year average of mass [ $\text{kg}/\text{m}^2$ ] 'clipped' in physics-dynamics coupling (so that state is not driven negative) when using `ftype=0` ('dribbling') physics-dynamics coupling for (a) water vapor, (b) cloud liquid and (c) cloud ice, respectively. Interestingly the element boundaries systematically show in the plots which is likely related to the anisotropy of the quadrature grid [Herrington *et al.*, 2018].